Saudi Journal of Biological Sciences 28 (2021) 386–394

Contents lists available at ScienceDirect

Saudi Journal of Biological Sciences

journal homepage: www.sciencedirect.com

Original article

$ZnCl_2$ catalyzed new coumarinyl-chalcones as cytotoxic agents

Konidala Sathish Kumar [a,b], Vijay Kotra [c,*], Phani Kumar Kola [h], CH.B. Praveena Devi [d], Nutakki Anusha [a], Bollikolla Hari Babu [e], Syed Farooq Adil [f,*], Mohammed Rafi Shaik [f], Mujeeb Khan [f], Abdulrahman Al-Warthan [f], Osamah Alduhaish [f,*], M. Mujahid Alam [g]

[a] Department of Pharmaceutical Chemistry, University College of Pharmaceutical Sciences, Acharya Nagarjuna University, Nagarjuna Nagar, Guntur 522510, India
[b] Department of Pharmaceutical Sciences, Vignan's Foundation for Science, Technology, and Research, Guntur, Andhra Pradesh, India
[c] Department of Pharmaceutical Chemistry, Faculty of Pharmacy, Quest International University Perak, 30250 Ipoh, Malaysia
[d] Department of Pharmacy, Joginpally B.R. Pharmacy College, Yenkapally, Moinabad Mandal, Hyderabad, Telangana 500075, India
[e] Department of Chemistry, University College of Sciences, Acharya Nagarjuna University, Nagarjuna Nagar, Guntur 522510, India
[f] Department of Chemistry, College of Science, King Saud University, P.O. Box 2455, Riyadh 11451, Saudi Arabia
[g] Department of Chemistry, College of Science, King Khalid University, Abha, Saudi Arabia
[h] Department of Pharmacology, University College of Pharmaceutical Sciences, Acharya Nagarjuna University, Nagarjuna Nagar, Guntur 522510, India

ARTICLE INFO

Article history:
Received 26 August 2020
Revised 12 October 2020
Accepted 14 October 2020
Available online 22 October 2020

Keywords:
Coumarinyl chalcones
Anti-cancer
Docking
Tyrosine kinase

ABSTRACT

A new series of coumarin-yl-chalcone derivatives (**3a-m**) had been designed and synthesized through different reactions such as aromatic addition, cyclization and Claisen-Schmidt reactions in good yields (54–78%). 5-acetyl-4-(2-hydroxyphenyl) -6-methyl-3, 4-dihydropyrimidin-2(1H) -one **(1)** has been synthesized by multi-component one pot reaction of salicylaldehyde, methyl acetoacetate and urea, which was further reacted with malonic acid employing $ZnCl_2$ catalyst to yield 5-acetyl-4-(4-hydroxy-2-oxo-2*H*-chromen-8-yl) -6-methyl-3, 4-dihydropyrimidin-2(1*H*) -one **(2).** The title compounds (**3a-m)** were synthesised by reacting 5-acetyl-4-(4-hydroxy-2-oxo-2*H*-chromen-8-yl) -6-methyl-3, 4-dihydropyrimidin-2(1*H*)-one (**2**) with different aromatic aldehydes in the presence of potassium hydroxide. *In silico* studies, a preliminary screening method for predicting the anti-cancer activity was performed for the synthesized compounds (**3a-m)** against Src, Alb tyrosine kinase and homology model protein (PDB ID: 4csv). The derivatives **3h** and **3m** showed moderate binding energies. The *in vitro* cytotoxic activity was evaluated for the compounds **3h** and **3m** by using human cancer cell-line morphology and MTT assay against three human cell-lines A549 (Lung), Jurkat (Leukemia) and MCF-7 (Breast). The results indicate that the derivatives **3h** and **3m** display significant anti-cancer activity, however it was found to be less cytotoxic when compared to the standard used i.e. Imatinib.

1. Introduction

Many medicinal plants are known to have unique anticarcinogenic, anti-inflammatory, and growth-modulatory effects on the cancer cells (Awan et al., 1908; Shaik et al., 2019; Vaidyanathan et al., 2019). Among them, Coumarin, a benzopyrone class of heterocyclic compound, are pharmacologically important compounds, mostly obtained from natural sources mostly higher plants (Venugopala et al., 2013). Most natural coumarins are oxygenated at C-7; Umbelliferone (7-hydroxycoumarin) being regarded as the structural and biogenetic parent of the more highly oxygenated coumarins (Intekhab and Aslam, 2009). Coumarin and its derivatives were reported to have innumerable pharmacological activities like anti-HIV (Shikishima et al., 2001), anti-tubercular (Karalı et al., 2002), anti-microbial (Kamal et al., 2009), anti-Alzheimer's (Anand et al., 2012; Piazzi et al., 2008), analgesic anti-inflammatory (Ghate et al., 2005), anti-cancer (Kamal et al., 2010), anti-hyperlipidemic (Madhavan et al., 2003), anti-hypertensive activity (Baek et al., 2000), anti-oxidant (Kharasch et al., 2000), neuroprotective activity (Wang et al., 2012), anti-diabetic (Tegginamath et al., 2016), anti-neurodegenerative (Jameel et al., 2016), anti-psychotics (Chen et al., 2013; Di Carlo

* Corresponding authors.
E-mail addresses: vijay.kotra@qiup.edu.my (V. Kotra), sfadil@ksu.edu.sa (S.F. Adil), oalduhaish@ksu.edu.sa (O. Alduhaish).
Peer review under responsibility of King Saud University.

Production and hosting by Elsevier

https://doi.org/10.1016/j.sjbs.2020.10.020
1319-562X/

et al., 1999), anti-coagulant (Sashidhara et al., 2012) activities. However, it was coupled with another class of naturally occurring pharmacologically important compounds chalcones (1,3-diaryl-2-propane-1-ones), which are secondary metabolites obtained from flavonoids and isoflavonoids mostly isolated from fruits, vegetables, spices, tea and soya-based foodstuff (Rozmer and Perjési, 2016). These chalcones have been reported to possess various beneficial biological properties including anti-bacterial, anti-fungal, anti-malarial, anti-HIV, anti-cancer, antioxidant, anti-tubercular (Kotra et al., 2010; Singh et al., 2014) activities.

Existing scientific literature describes that different types of coumarinyl chalcones are designed, screened for anti-cancer activity against different types of target proteins like tubulin, Falcipian-2 (Pingaew et al., 2014), Cdc25 (Valente et al., 2010) by *in-silico* screening, screened for anti-cancer activity by in-vitro Glutathione-S-transferase Cdc25 recombinant enzyme assay, screened for anti-cancer activity by *in vitro* method on different human cancer cell lines like oral, cervical, breast, lung, hepatic, lymph, leukaemia, pancreatic, Nasopharyngeal (Wei et al., 2016).

Another class of compounds, dihydropyrimidinones, has been found to possess a variety of biological activities such as anti-inflammatory, calcium channel antagonism/inhibition other than antitumoral activity, especially after the discovery of the compound monastrol, a dihydropyrimidinone, with Eg5 kinesin inhibitor efficiency (Beena et al., 2016; Vijay et al., 2010). The enzymes tyrosine kinases like Protein Tyrosine kinases, receptor tyrosine kinases (RTKs), Src, a mutant variant protein of tyrosine kinase, Alb tyrosine kinases and non-receptor tyrosine kinases (NRTKs) are the few enzymes responsible for cell proliferation, migration, differentiation and survival. The mutations or over expression of tyrosine kinase leads to uncontrolled cell growth through progressive or uncontrolled activation of intracellular pathway cascades. The relationship between the receptor tyrosine kinase and the cancer development was revealed by many scientific researches (Paul and Mukhopadhyay, 2004).

The modern drug development strategy for anti-cancer activity includes *in-silico* docking of new molecules on different target proteins (Viana et al., 2018). Tyrosine kinases are considered as targets in cancer chemotherapy due to the vital role in altering the growth factor signalling pathway. This paper explains the design and synthesis of some new dihydropyrimidinone substituted coumarinyl chalcones (Scheme 1) by hybridization-based on their docking score obtained by the *in-silico* studies. The synthesized derivatives were subjected to spectral characterization along with *in-vitro* anti-cancer studies, using Imatinib, a highly effective non-receptor tyrosine kinase inhibitor, as standard.

2. Experimental

2.1. Materials, methods and characterization

The chemicals and materials used in this work. The chemicals used for synthesis were purchased urea was purchased from Loba Chemie Pvt. Ltd., India, 2-hydroxybenzaldehyde was obtained from Fisher Scientific, UK, pentane-2,4-dione was purchased from Merck, Germany and Avra Synthesis Pvt. Ltd. *In-silico* molecular docking was performed by using Chem office 2016 and VLifeMDS. Melting points of synthesized compounds were determined by Dalal Melting Point Apparatus using open capillary tubes. Infrared spectra were recorded using the KBr Pellet method. ^{1}H NMR and ^{13}C NMR spectra were determined by using Bruker-NMR Spectrometer 400 MHz. Mass spectra were measured with Shimadzu GCMS QP 5000 mass spectrometer. Other chemicals were of commercial grade and used without further purification. The homogeneity of the compounds was checked by thin-layer chromatography (TLC) on TLC silica gel F_{254}aluminum plates (E. Merck, Germany) using chloroform-methanol (3:1) mixture as mobile phase and visualized using iodine vapors.

Completion of synthetic reactions and purity of end products of reactions were confirmed by Thin Layer Chromatography on TLC silica gel F_{254}aluminum plates (E. Merck, Germany), using acetone and ethyl acetate as mobile spots are visualized with UV chamber and iodine vapors.

2.2. General procedure for synthesis of 5-acetyl-4-(2-hydroxyphenyl) -6-methyl-3,4-dihydropyrimidin-2(1H) -one (**1**)

A mixture of Salicylaldehyde (1 mmol), Methyl acetoacetate (1.1 mmol), urea (1.3 mmol) and citric acid (0.5 mmol) was taken into a round bottom flask, heated at 80 °C under stirring. Completion of the reaction was monitored by TLC. To the reaction mixture, cold water was added and stirred for 10 min, then filtered, washed with water, dried in vacuum and the obtained product was further recrystallized from ethanol. white crystals; yield 85.41%; m.p. 112–114 °C; IR (KBr, cm^{-1}): v 3479(N—H), 3370(O—H), 3060 (C—H Ar), 2925(C—H), 1734(C=O), 1671(C=O); ^{1}H NMR (400 MHz, DMSO d_6,

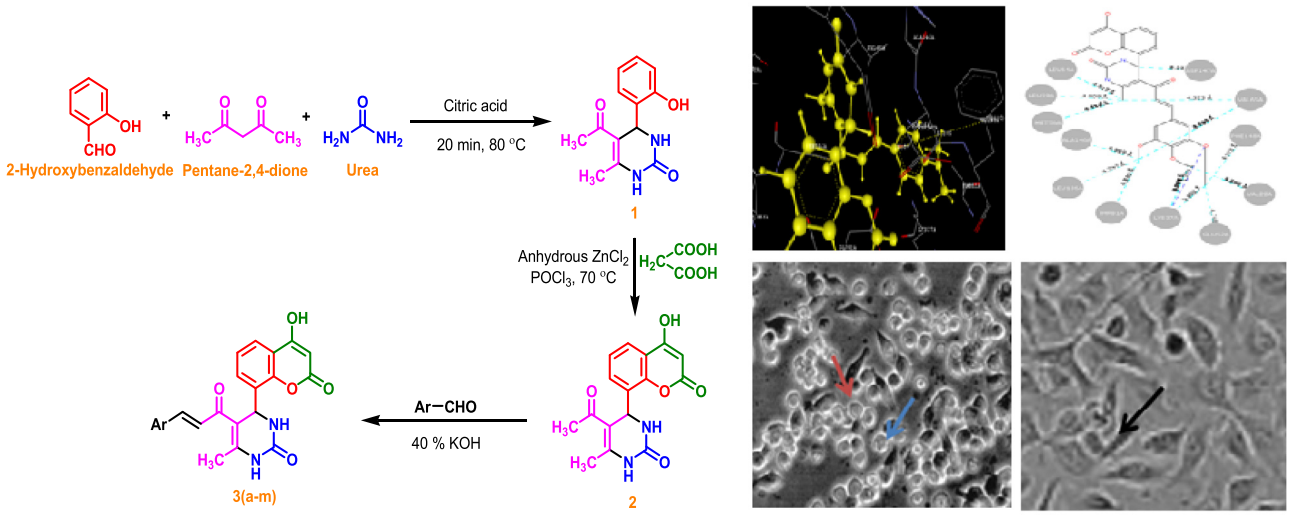

Scheme 1. Schematic representation of dihydropyrimidinone derived coumarinyl chalcones.

δ/ppm): 2.28(s, 3H, CH), 2.35(s, 3H, CH—C═O), 4.91 (s, H, CH), 6.83–7.86 (m, 5H, aromatic), 9.03 (s, H, NH), 9.71 (s, H, OH). ^{13}C NMR (100 MHz, DMSO d_6) δ/ppm: 19.4 (CH_3), 27.3 (CH_3), 41.8 (CH), 106.2, 121.6, 122.3, 128.7 (Ar—C), 145.4 (C—N), 150.7 (C═O), 154.2 (C—O), 192.5 (C═O). MS (*m*/*z*, (relative abundance, %): 247 (M + 1, 14.8), 203 (M+, 33.2), 154 (M+, 100), 94 (M+, 27).

*2.3. General procedure for synthesis 5-acetyl-4-(4-hydroxy-2-oxo-2H-chromen-8-yl) -6-methyl-3,4-dihydropyrimidin-2(1H) -one (**2**)*

A mixture of 5-acetyl-4-(2-hydroxyphenyl) -6-methyl-3,4-dihy dropyrimidin-2(1H)-one (0.1 mol) and malonic acid (0.1 mol) was added to a mixture of phosphorus oxychloride (40 mL) and anhydrous zinc chloride (30 g) which was preheated to 60–70 °C and the reaction mixture was heated on a water bath at 70 °C for 20 h. Completion of the reaction was monitored by TLC, then cool and pour the mixture in ice-cold water to afford a solid, washed with cold water and then filtered. It was then treated with 10% sodium carbonate solution and then filtered. The filtrate was slowly acidified with diluted hydrochloric acid. The product was filtered and washed with water and further dried and recrystallized from glacial acetic acid. Brick red crystals; yield 72.45%; m. p. 102–104 °C; IR (KBr, cm^{-1}): v 3456(N—H), 3362(O—H), 3038 (C—H Ar), 2928(C—H), 1732(C═O), 1665(C═O); 1H NMR (400 MHz, DMSO d_6, δ/ppm): 2.23(s, 3H, CH), 2.32 (s, 3H, CH), 5.09 (s, H, CH), 6.82–7.69 (m, 5H, aromatic), 9.06 (s, H, NH), 9.88 (s, H, OH). ^{13}C NMR (100 MHz, DMSO d_6) δ/ppm: 19.7 (CH_3), 27.4 (CH_3), 42.3(C—CH), 91.6, 106.2, 117.2, 121.3, 125.2, 126.5, 128.2, (Ar—C), 145. 1 (C—N), 192.3 (C═O), 150.2 (C═O), 162.1 (C═O), 166.8 (C—O). MS (*m*/*z*, (relative abundance, %): 315 (M + 1, 18.1), 271 (M+, 36), 154 (M+, 100), 162 (M+, 41).

*2.4. General procedure for synthesis of coumarinyl-chalones (**3a-m**)*

Dissolve 0.002 mol of 5-acetyl-4-(4-hydroxy-2-oxo-2H-chro men-8-yl) -6-methyl-3,4-dihydropyrimidin-2(1H) -one and 0.002 mol of substituted aromatic aldehyde in 6 mL of ethanol. While stirring, add 3 mL of 40% KOH dropwise and continue the stirring for about 30 h as this will be similarity throughout the manuscript.rs. Completion of the reaction was monitored by TLC. Then add crushed ice to the mixture add to neutralize the mixture with dil. HCl to get precipitate. Recrystallize the product obtained from ethanol.

*2.4.1. 5-cinnamoyl-4-(4-hydroxy-2-oxo-2H-chromen-8-yl) -6-methyl-3,4-dihydropyrimidin-2(1H) -one (**3a**)*

The was found to be Yellow crystals; yield 65.41%; m.p. 153–155 °C; IR (KBr, cm^{-1}): v 3479(N—H), 3370(O—H), 3060 (C—H Ar), 2925(C—H), 1734(C═O), 1671(C═O); 1H NMR (400 MHz, DMSO d_6, δ/ppm): 2.50(s, 3H, CH), 4.95(s, H, CH), 6.9–7.65 (m, 13H, aromatic), 9.13(s, H, NH). ^{13}C NMR (100 MHz, DMSO d_6) δ/ppm: 17.7 (CH_3), 42.5(C—CH), 117.4, 121.3, 125.2, 126.5, 127.9, 128.4, 128.5, 128.6, 135.2, 148.3, 154.8 (Ar—C), 193.3 (C═O), 150.2 (C═O), 162.2 (C═O), 166.1(C—O), 142.2 (C═C). MS (*m*/*z*, (relative abundance, %)): 403 (M + 1, 25.6), 271 (47), 243 (M + 2, 100), 162 (M+, 54), 132 (36).

*2.4.2. (E) -4-(4-hydroxy-2-oxo-2H-chromen-8-yl) -5-(3-(4-methoxyphenyl) acryloyl) -6-methyl-3,4-dihydropyrimidin-2(1H) -one (**3b**)*

Dark red crystals; yield 62.76%; m.p. 168–170 °C; IR (KBr, cm^{-1}): v3436(N—H), 3362(O—H), 3038 (C—H Ar), 2928(C—H), 1732(C═O), 1665(C═O), 758 (o-sub); 1H NMR (400 MHz, DMSO d_6, δ/ppm): 2.54(s, 3H, CH), 3.78 (s, 3H, CH), 4.91(s, H, CH), 6.9–7.84 (m, 12H, aromatic), 9.11(s, H, NH). ^{13}C NMR (100 MHz, DMSO d_6) δ/ppm: 17.9 (CH_3), 42.2(C—CH), 54.3(CH), 91.4, 114.4, 117.6, 118.2, 121.1, 123.7, 125.6, 126.1, 127.3, 128.7, 130.4, 154.3, 159.2 (Ar—C), 193.5 (C═O), 150.4 (C═O), 162.6 (C═O), 166.5(C—O), 142.6 (C═C). MS (*m*/*z*, (relative abundance, %): 433 (M + 1, 26.4), 327 (M + 2, 100), 272 (M+, 36), 162 (M+, 28), 108 (57).

*2.4.3. 4-(4-hydroxy-2-oxo-2H-chromen-8-yl) -6-methyl-5-((2E,4E) -5-phenylpenta-2,4-dienoyl) -3,4-dihydropyrimidin-2(1H) -one (**3c**)*

Yellow crystals; yield 72.28%; m.p. 151–152 °C;): IR (KBr, cm^{-1}):v3462(N—H), 3269(O—H), 3027 (C—H Ar), 2923(C—H), 1739(C═O), 1674(C═O), 758(Ar); 1H NMR (400 MHz, DMSO d_6, δ/ppm): 2.48(s, 3H, CH), 4.74 (s, H, CH), 6.6–7.75 (m, 15H, aromatic), 9.05 (s, H, NH). ^{13}C NMR (100 MHz, DMSO d_6) δ/ppm: 17.6 (CH_3), 42.1(C—CH), 91.2, 117.3, 118.5, 121.5, 125.4, 126.3, 127.2, 128.3, 128.6, 135.4, 154.2 (Ar—C), 193.2 (C═O), 150.1 (C═O), 162.4 (C═O), 166.6 (C—O), 141.3 (C═C), 151.4 (C═C). MS (*m*/*z*, (relative abundance, %): 429 (M + 1, 27.5), 327 (M + 2, 100), 272 (M+, 36), 162 (M+, 28), 108 (57).

*2.4.4. (E) -4-(4-hydroxy-2-oxo-2H-chromen-8-yl) -6-methyl-5-(3-(2-nitrophenyl) acryloyl) -3,4-dihydropyrimidin-2(1H) -one (**3d**)*

Green crystals; yield 57.37%; m.p. 117–1119 °C;): IR (KBr, cm^{-1}): v3445(N—H), 3378(O—H), 3042(C—H Ar), 2927(C—H), 1741(C═O), 1672(C═O), 1531,1384 (Nitro), 756 (p-sub); 1H NMR (400 MHz, DMSO d_6, δ/ppm): 2.49(s, 3H, CH), 4.93 (s, H, CH), 7.10–8.39 (m, 12H, aromatic), 9.09 (s, H, NH). ^{13}C NMR (100 MHz, DMSO d_6) δ/ppm: 18.3 (CH_3), 42.7 (C—CH), 91.2, 117.5, 118.2, 121.1, 123.2, 123.6, 125.1, 126.8, 128.1, 128.4, 134.2, 154.1 (Ar—C), 193.5 (C═O), 150.5 (C═O), 162.8 (C═O), 166.3 (C—O), 147.3 (C—N), 152.6 (C═C). MS (*m*/*z*, (relative abundance, %): 448 (M + 1, 25.3), 325 (M + 2, 100), 272 (M+, 36), 162 (M+, 28), 108 (57).

*2.4.5. (E) -4-(4-hydroxy-2-oxo-2H-chromen-8-yl) -5-(3-(4-hydroxyphenyl) acryloyl) -6-methyl-3,4-dihydropyrimidin-2(1H) -one (**3e**)*

Brown crystals; yield 66.18%; m.p. 127–129 °C; IR (KBr, cm^{-1}): v3469(N—H), 3274(O—H), 3056(C—H Ar), 2936(C—H), 1729(C═O), 1670(C═O), 758 (o-sub); 1H NMR (400 MHz, DMSO d_6, δ/ppm): 2.27(s, 3H, CH), 4.88(s, H, CH), 6.78–8.17 (m, 12H, aromatic), 9.02 (s, H, NH), 9.56 (s, H, OH). ^{13}C NMR (100 MHz, DMSO d_6) δ/ppm: 17.95 (CH_3), 43.3(C—CH), 115.2, 117.6, 118.7, 121.7, 123.5, 125.5, 126.3, 127.4, 128.7, 130.4, 154.3 (Ar—C), 193.5 (C═O), 150.1 (C═O), 162.2 (C═O), 166.7 (C—O), 142.6 (C═C), 157.2 (C═O). MS (*m*/*z*, (relative abundance, %): 419 (M + 1, 27.3), 326 (M+, 37), 272 (M+, 100), 147 (M+, 41), 106 (23).

*2.4.6. (E) -4-(4-hydroxy-2-oxo-2H-chromen-8-yl) -6-methyl-5-(3-(4-nitrophenyl) acryloyl) -3,4-dihydropyrimidin-2(1H) -one (**3f**)*

Brown crystals; yield 54.29%; m.p. 173–174 °C; IR (KBr, cm^{-1}): v3479(N—H), 3113(O—H), 3081(C—H Ar), 2927(C—H), 1763(C═O), 1692(C═O), 1522,1345 (Nitro), 758 (o-sub); 1H NMR (400 MHz, DMSO d_6, δ/ppm): 2.42(s, 3H, CH), 4.75(s, H, CH), 7.05–8.30 (m, 12H, aromatic), 9.05 (s, H, NH). ^{13}C NMR (100 MHz, DMSO d_6) δ/ppm: 20.13 (CH_3), 45.6(C—CH), 95.2, 117.9, 118.1, 121.9, 123.5, 124.3, 125.7, 126.8, 128.6, 129.2, 130.1, 141.5, 148.5, 154.2 (Ar—C), 193.6 (C═O), 150.5 (C═O), 162.4 (C═O), 166.4 (C—O), 142.3 (C═C). MS (*m*/*z*, (relative abundance, %): 448 (M + 1, 27.3), 326 (M+, 28), 272 (M+, 100), 177 (M+, 19), 123 (31).

*2.4.7. (E) -5-(3-(4-chlorophenyl) acryloyl) -4-(4-hydroxy-2-oxo-2H-chromen-8-yl) -6-methyl-3,4-dihydropyrimidin-2(1H) -one (**3g**)*

Golden yellow crystals; yield 78.72%; m.p. 182–184 °C; IR (KBr, cm^{-1}): v3438(N—H), 3238(O—H), 3062(C—H Ar), 2928(C—H), 1732 (C═O), 1672(C═O), 758 (o-sub); 1H NMR (400 MHz, DMSO d_6, δ/ppm): 2.49 (s, 3H, CH), 4.92 (s, H, CH), 7.03–7.75 (m, 12H, aromatic), 9.09 (s, H, NH). ^{13}C NMR (100 MHz, DMSO d_6) δ/ppm:

20.4 (CH_3), 43.2 (C—CH), 92.1, 117.2, 118.7, 121.5, 123.1, 125.5, 126.2, 128.3, 129.2, 129.9, 133.5, 133.9, 148.5, 154.4 (Ar—C), 193.3 (C=O), 150.1 (C=O), 162.8 (C=O), 166.7 (C—O), 143.5 (C=C). MS (*m*/*z*, (relative abundance, %): 438 (M + 2, 32.1), 326 (M+, 37), 272 (M+, 100), 162 (M+, 26), 111 (41).

*2.4.8. (E) -5-(3-(4-(dimethylamino) phenyl) acryloyl) -4-(4-hydroxy-2-oxo-2H-chromen-8-yl) -6-methyl-3,4-dihydropyrimidin-2(1H) -one (**3h**)*

Dark brown crystals; yield 58.38%; m.p. 144–146 °C; IR (KBr, cm^{-1}): v3402(N—H), 3225(O—H), 3032(C—H Ar), 2925(C—H), 1713(C=O), 1668(C=O), 765(o-sub); 1H NMR (400 MHz, DMSO d_6, δ/ppm): 2.47 (s, 3H, CH), 3.10 (s, 6H, CH), 5.05 (s, H, CH), 6.50–7.95 (m, 12H, aromatic), 9.05 (s, H, NH). ^{13}C NMR (100 MHz, DMSO d_6) δ/ppm: 20.7 (CH_3), 40. 2 (N—CH), 45.1 (C—CH), 92.5, 117.6, 118.2, 121.7, 123.4, 124.4, 125.1, 126.5, 128.7, 129.1, 148.2 (Ar—C), 150.6, 154.4 (Ar—C—N), 193.6 (C=O), 150.4 (C=O), 162.2 (C=O), 166.3 (C—O), 142.1 (C=C). MS (*m*/*z*, (relative abundance, %): 446 (M + 1, 27.5), 326 (M+, 28), 272 (M+, 100), 174 (M+, 15), 120 (32).

*2.4.9. (E) -4-(4-hydroxy-2-oxo-2H-chromen-8-yl) -5-(3-(2-hydroxyphenyl) acryloyl) -6-methyl-3,4-dihydropyrimidin-2(1H) -one (**3i**)*

Orange crystals; yield 68.83%; m.p. 155–157 °C; IR (KBr, cm^{-1}): v3452(N—H), 3234(O—H), 3062(C—H Ar), 2928(C—H), 1742(C=O), 1667(C=O), 757(p-sub); 1H NMR (400 MHz, DMSO d_6, δ/ppm): 2.38 (s, 3H, CH), 4.74 (s, H, CH), 6.72–8.21 (m, 12H, aromatic), 9.07 (s, H, NH), 11.21 (s, H, OH). ^{13}C NMR (100 MHz, DMSO d_6) δ/ppm: 20.2 (CH_3), 43.4 (C—CH), 91.3, 117.4, 118.6, 121.2, 122.2, 123.1, 125.6, 126.3, 128.2, 129.1, 129.5, 148.4 (Ar—C), 154.6 (Ar—C—N), 193.1 (C=O), 150.7 (C=O), 162.8 (C=O), 157.4, 166.7 (C—O), 152.4 (C=C). MS (*m*/*z*, (relative abundance, %): 419 (M + 1, 25.3), 326 (M+, 17), 272 (M+, 100), 162 (M+, 35), 94 (26).

*2.4.10. (E) -4-(4-hydroxy-2-oxo-2H-chromen-8-yl) -5-(3-(3-hydroxyphenyl) acryloyl) -6-methyl-3,4-dihydropyrimidin-2(1H) -one (**3j**)*

Yellow crystals; yield 53.11%; m.p. 136–138 °C; IR (KBr, cm^{-1}): v3458(N—H), 3237(O—H), 3046(C—H Ar), 2930(C—H), 1730(C=O), 1672(C=O), 757(m-sub);1H NMR (400 MHz, DMSO d_6, δ/ppm): 2.44 (s, 3H, CH), 5.03 (s, H, CH), 6.58–8.05 (m, 12H, aromatic), 9.07 (s, H, NH), 9.58 (s, H, OH). ^{13}C NMR (100 MHz, DMSO d_6) δ/ppm: 20.4 (CH_3), 45.2 (C—CH), 91.2, 115.3, 117.6, 117.8, 118.4, 121.2, 123.5, 125.1, 126.9, 128.4, 130.4, 148.2 (Ar—C), 154.3 (Ar—C—N), 193.4 (C=O), 150.2 (C=O), 162.3 (C=O), 158.2, 166.3 (C—O), 142.5 (C=C). MS (*m*/*z*, (relative abundance, %): 419 (M + 1, 25.3), 326 (M+, 17), 272 (M+, 100), 162 (M+, 35), 94 (26).

*2.4.11. (E) -4-(4-hydroxy-2-oxo-2H-chromen-8-yl) -6-methyl-5-(3-(3-nitrophenyl) acryloyl) -3,4-dihydropyrimidin-2(1H) -one (**3k**)*

Greenish white crystals; yield 59.73%; m.p. 103–105 °C; IR (KBr, cm^{-1}): v3385(N—H), 3238(O—H), 3049(C—H Ar), 2926(C—H), 1737 (C=O), 1673(C=O), 1489,1282 (nitro), 753(m-sub); 1H NMR (400 MHz, DMSO d_6, δ/ppm): 2.38 (s, 3H, CH), 4.89 (s, H, CH), 6.49–8.52 (m, 12H, aromatic), 9.07 (s, H, NH). ^{13}C NMR (100 MHz, DMSO d_6) δ/ppm: 17.8 (CH_3), 41.9 (C—CH), 92.4, 117.9, 118.1, 121.5, 123.8, 125.6, 126.9, 128.1, 130.1, 136.2, 137.9, 148.5 (Ar—C), 147.5, 154.3 (Ar—C—N), 193.2 (C=O), 150.6 (C=O), 162.1 (C=O), 166.7 (C—O), 142.7 (C=C). MS (*m*/*z*, (relative abundance, %): 448 (M + 1, 25.3), 326 (M+, 25), 272 (M+, 100), 177 (M+, 42), 123 (15).

*2.4.12. (E) -5-(3-(2-chlorophenyl) acryloyl) -4-(4-hydroxy-2-oxo-2H-chromen-8-yl) -6-methyl-3,4-dihydropyrimidin-2(1H) -one (**3l**)*

Browncrystals; yield 57.25%; m.p. 106–107 °C; IR (KBr, cm^{-1}): v3379(N—H), 3167(O—H), 3058(C—H Ar), 2926(C—H), 1739 (C=O), 1673(C=O), 757(p-sub); 1H NMR (400 MHz, DMSO d_6, δ/ppm): 2.41 (s, 3H, CH), 4.95 (s, H, CH), 6.81–8.20 (m, 12H, aromatic), 9.03 (s, H, NH). ^{13}C NMR (100 MHz, DMSO d_6) δ/ppm: 20.2 (CH_3), 42.3 (C—CH), 91.7, 117.7, 118.8, 121.3, 123.2, 125.2, 126.4, 127.3, 128.9, 129.1, 130.2, 133.2, 134.4, 148.1 (Ar—C), 154.3 (Ar—C—N), 193.2 (C=O), 150.2 (C=O), 162.6 (C=O), 166.3 (C—O), 122.2 (C=C), 134.5 (C—Cl). MS (*m*/*z*, (relative abundance, %): 438 (M + 2, 32.5), 326 (M+, 31), 272 (M+, 100), 166 (M+, 38), 112 (44).

*2.4.13. (E) -4-(4-hydroxy-2-oxo-2H-chromen-8-yl) -6-methyl-5-(3-(3,4,5-trimethoxyphenyl) acryloyl) -3,4-dihydropyrimidin-2(1H) -one (**3m**)*

Brick red crystals; yield 65.41%; m.p. 153–155 °C; IR (KBr, cm^{-1}): v3414(N—H), 3234(O—H), 3059(C—H Ar), 2939(C—H), 1737(C=O), 1675(C=O), 758, 645(3,4,5-sub); 1H NMR (400 MHz, DMSO d_6, δ/ppm): 2.47 (s, 3H, CH), 3.91 (s, 9H, CH), 4.78 (s, H, CH), 6.75–8.10 (m, 10*H*, aromatic), 9.08 (s, H, NH). ^{13}C NMR (100 MHz, DMSO d_6) δ/ppm: 20.5 (CH_3), 40.4 (C—CH), 56.5, 60.7 (O—CH_3), 92.4, 103.1, 117.3, 118.5, 121.6, 123.5, 125.7, 126.3, 128.7, 148.5 (Ar—C), 154.5 (Ar—C—N), 193.6 (C=O), 150.7 (C=O), 162.4 (C=O), 138.5, 153.1, 166.3 (C—O), 142.5 (C=C). MS (*m*/*z*, (relative abundance, %): 493 (M + 1, 28.7), 326 (M+, 45), 272 (M+, 100), 223 (M+, 27), 168 (32).

2.5. Docking studies

Docking study was performed for the evaluation of the anticancer activity of synthesized derivatives **3a-m** against tyrosine kinase protein (4csv) using VLife MDS software. The ligands were prepared by the VLife engine tool. The X-ray crystal structure of protein tyrosine kinase (4csv) was downloaded from rcsb.com/pdb site. The protein crystal structure optimized by removal of water molecules, addition hydrogen, Ramachandran plot analysis using Biopredicta module tolls of VLifeMDS. To identify the co-crystal ligand bound to the amino acid sequence of the protein, save the protein structure and the extracted co-crystal ligand in mol2 format, which can be used as reference ligand. The grid docking was performed using GRIP docking under batch docking option in the Biopredicta module**.** The interpretation of the result was done based on the score obtained by conformers of the ligands. The conformer which has the least score should be the one which has the high binding energy to the active site in the protein. We can examine the interaction between the ligand and protein by selecting the different scoring options like hydrogen bond, hydrophobic interaction π-stacking, and van der Waals force, etc.

2.6. In vitro anticancer activity

The anticancer activity was evaluated for compounds **3h** and **3m** by *in vitro* methods using morphology and MTT assay against Human malignant cell lines like A549 (Lung), Jurkat (Leukemia) and MCF-7 (Breast). A549, Jurkat and MCF-7 cells were sub-cultured in-house, in PGP Life Sciences, Hyderabad. The source of the cell line is ATCC. Cells were grown in 75 cm^2 bottle canted necked vented flasks (Corning) with RPMI and the cells were maintained in a humidified atmosphere of 5% CO_2 at 37 °C. Cells (passages 25–35) were grown in Dulbecco's Modified Eagles medium (Gibco Invitrogen, Paisley, UK) supplemented with 10% fetal bovine serum, 1% non-essential amino acids, 1% penicillin (1000U/mL), 1% streptomycin (1000 μg/mL) and 1% amphotericin (250 U/mL). The cells were passaged enzymatically with 0.25% trypsin- 1 mM EDTA and sub-cultured on 75 cm^2 plastic flasks at a density of 2.2 × 104 cells/cm^2. The culture medium was replaced every 2 days. Subculturing was done by briefly rinsed the cell layer with 0.25% (w/v) Trypsin- 0.53 mM EDTA solution to remove all traces of serum that

contains trypsin inhibitor after Removing and discarding culture medium. 2.0–3.0 mL of Trypsin-EDTA solution was added to the flask and observed, cells under an inverted microscope until cell layer is dispersed (usually within 5–15 min). 6.0–8.0 mL of complete growth medium was added and aspirated the cells by gently pipetting. Appropriate aliquots of the cell suspension were added to new culture vessels. Cultures can be established between 2 × 103 and 1 × 104 viable cells/cm^2. Do not exceed 7 × 104 cells/cm^2. Cultures were incubated at 37 °C.

The morphology was done by the subcultured human cell lines, Jurkat, A549 and MCF-7 cells were treated 12 h post-seeding with 150 & 300 mg/mL concentration of **3h** and **3m** for morphological study. Cells were observed for 24, 48 and 72 h, after treatment of test samples. Cell confluence (80%) was confirmed by microscopic observance. Images were taken by the Axiovert 200 M phase-contrast microscope at the magnification of 10x. Axiovision Rel.4.2 software was used to acquire the images.

The MTT assay was performed by inoculating cultured Jurkat, A549 and MCF-7 cells (100 μL per well) in a clear bottom 96-well tissue (abdos) culture plates (The number of cells was 10^5 cells per well). All three cell lines Jurkat, A549, and MCF-7 were used for **3h**; A549 and Jurkat cell lines were used for **3m** to determine IC_{50} of their cytotoxicity. The compounds **3h** and **3m** were added in different concentrations ranging from 10 to 150 μg/mL (10, 25, 50, 75, 100, 125 and 150 μg/mL) in triplicate after 24 h of seeding and incubated the cells for 24 h, 48 h and 72 h period of time. A volume of 20 μL culture medium was used for all test samples. Remove the medium and wash the cell twice with PBS. Add 15 μL MTT reagent per well which was made up in PBS medium to a final concentration of 0.5 mg/mL. The volume of the reagent should be adjusted depending on the volume of the cell culture. Cells were incubated for 3 h at 37 °C until intracellular purple formazan crystals are visible under the microscope. MTT reagent removed and 100 μL of the DMSO was added to each well and mixed gently on an orbital shaker for one hour at room temperature. The volume of DMSO should be adjusted depending on the volume of cell culture. The absorbance was measured at 570 nm for each well on an absorbance plate reader and IC_{50} values were calculated. A positive control Imatinib was used as a known cytotoxic activity agent. Dimethyl sulfoxide was the vehicle used for dissolution of the testing compound, and its final concentration on the cells was less than 0.2%.

3. Results

3.1. Chemistry

Dihydropyrimidinone derived coumarinyl chalcones were synthesised according to the reported protocols (Scheme 2).

Briefly, the dihydropyrimidinone (1) was obtained by one pot synthesis from 2 hydroxy-benzaldehyde, pentane 2, 4 dione, urea using citric acid as catalyst. The obtained 2-hydroxy dihydropyrimidinone derivatives were then treated with malonic acid in presence of anhydrous $ZnCl_2$. Finally, the obtained Dihydropyrimidino coumarins were treated with various aromatic aldehydes to yield the titled compounds **(3a-m).**

The results had shown that the compounds were fitted into the active pocket by forming hydrogen bonding, hydrophobic and π-stacking interactions with amino acids of tyrosine protein were shown in Figs. 1 and 2. The docked compounds binding energies

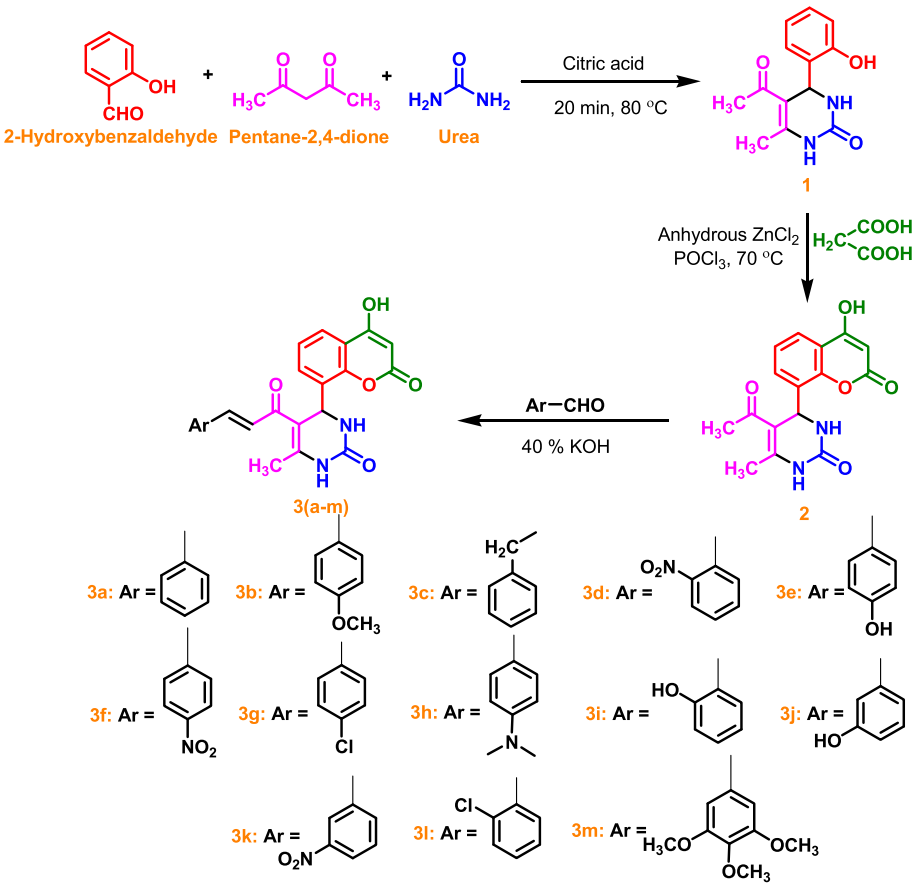

Scheme 2. Synthesis of compounds **3(a-m)**.

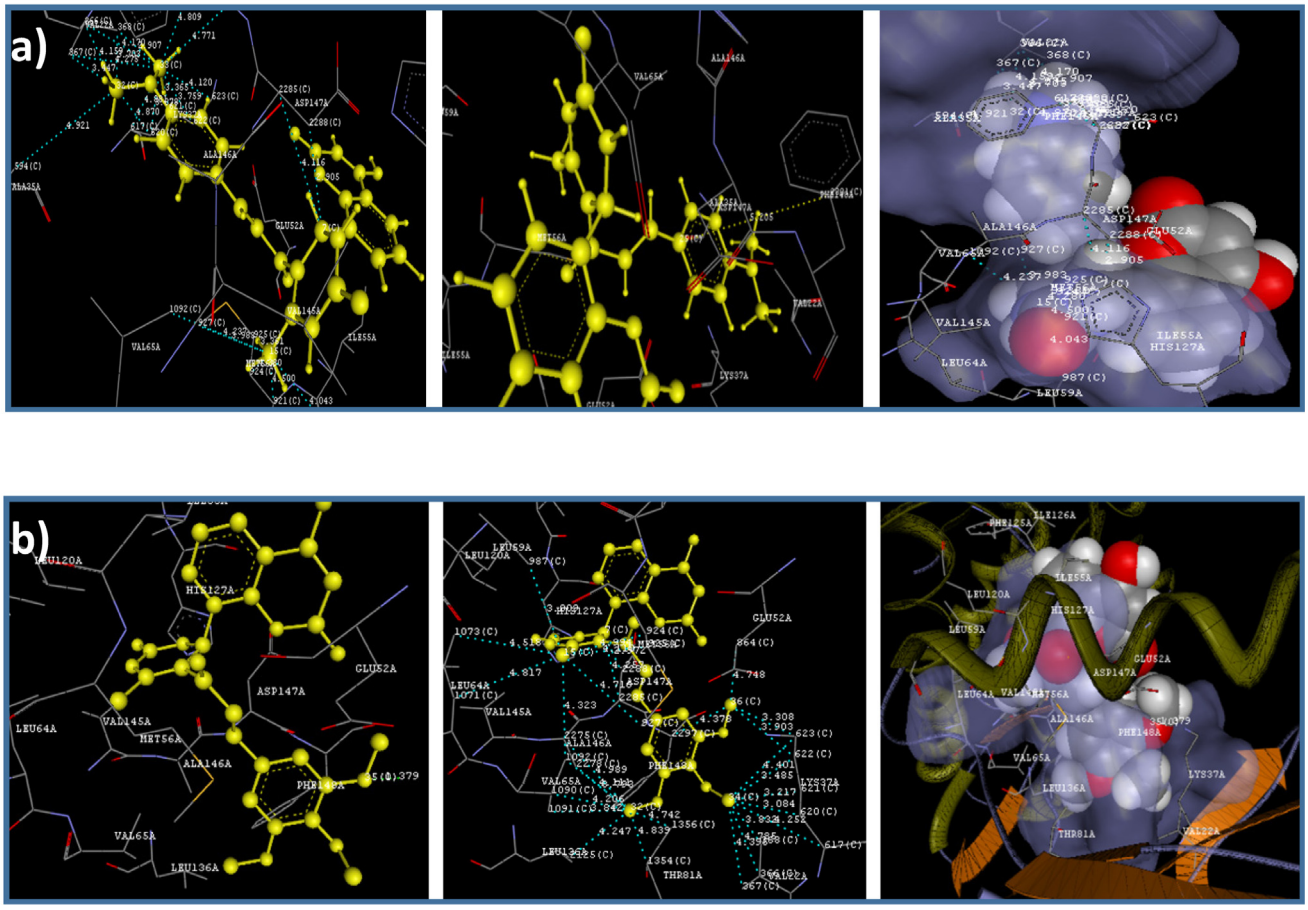

Fig. 1. Docking interactions 2D view: a) π-stacking interaction and hydrophobic interaction of derivative **3h;** b) Hydrogen bonding and Hydrophobic of derivative **3m**.

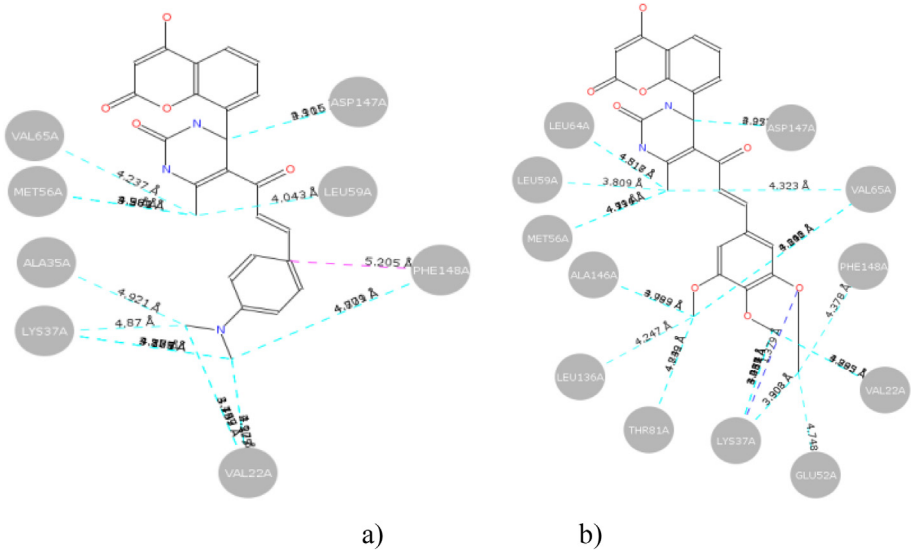

Fig. 2. Docking interactions 3D view: a) π-stacking interaction (Blue) and Hydrophobic interaction (Grey) of derivative **3h**; b) Hydrogen bonding (Blue) and Hydrophobic (Grey) of derivative **3m**.

are exhibited in Table 1. The microscopic images displaying the morphological changes in cancer cell upon treatment with the compounds **3h** and **3m** are depicted in Fig. 3. Based on the morphological studies, we conducted the MTT assay for **3h** against Jurkat, A549, and MCF-7 and **3m** against Jurkat and A549 human cell-lines. The anti-cancer activity of compounds 3h and 3m are shown in Table 2. These obtained results are comprehensively explained below in the discussion section.

Table 1
Binding energies of docked compounds.

S. No.	Compound	Binding energy
1	**3h**	**−60.162**
2	**3m**	**−50.521**
3	**3f**	**−46.002**
4	**3k**	**−44.220**
5	**3a**	**−12.586**
6	**3i**	**0.475**
7	**3c**	**31.794**
8	**3l**	**66.242**
9	**3d**	**67.660**
10	**3j**	**69.478**
11	**3g**	**–**
12	**3b**	**–**
13	**3e**	**–**
14	**Imatinib**	**−118.260**

3.2. Discussions

3.2.1. Molecular docking

The title compounds (**3a-m**) were docked into the active pocket of Src, Albtyrosine kinase homology model protein (PDB ID: 4csv) co-crystallized with Imatinib standard drug for elucidating the anti-cancer activity. The docking was performed by utilizing VLife MDS software to observe the binding interaction as docking score. Among all the derivatives synthesized, **3h** and **3m** had shown moderate interaction with docking scores as −60.162 and −50.521 respectively when compared to Imatinib docking score −118.26. The results had shown in Fig. 1& 2. indicating that the compounds were fitted into the active pocket by forming hydrogen bonding, hydrophobic and π-stacking interactions with amino acids of tyrosine protein. The derivative **3h** has the π-stacking interaction between B ring of chalcone moiety and PHE148, Hydrophobic bond with ASP147, VAL65, MET65, LEU59, AL35, LYS37, PHE148, and VAL22. The derivative **3m** has the Hydrogen bond interaction between the oxygen of parametoxy and LYS37

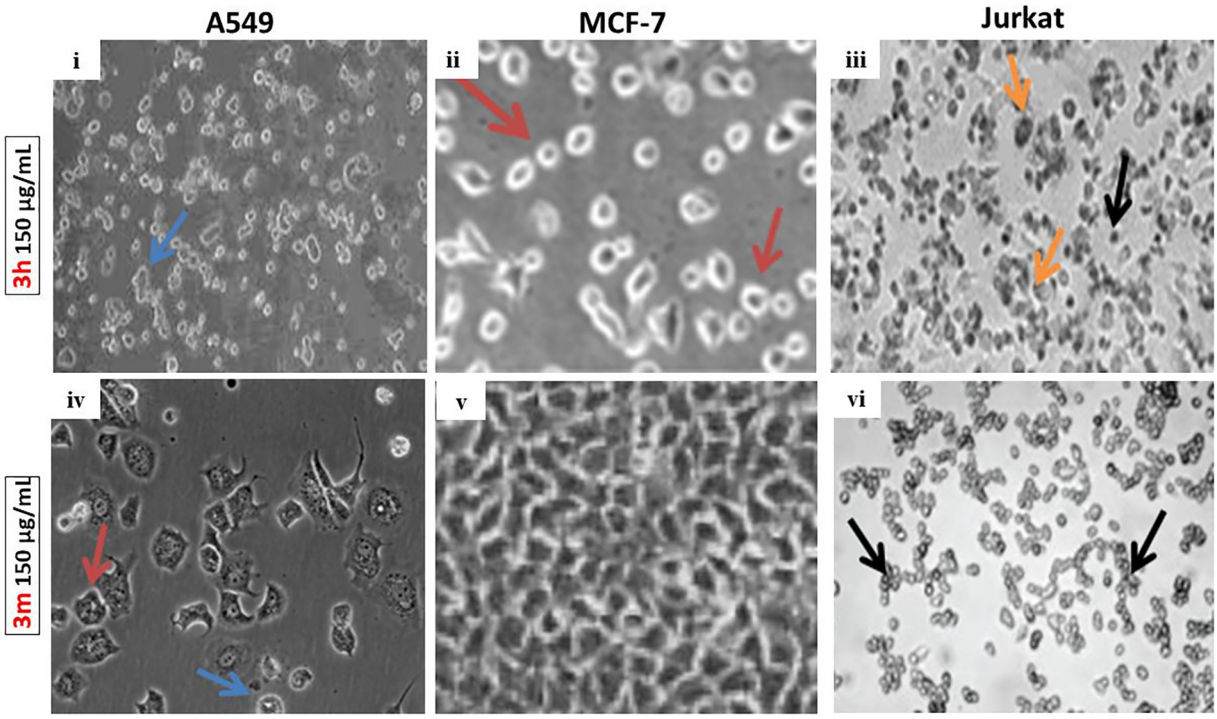

Fig. 3. Digital microscopic images of morphological changes in cancer cell upon treatment with the compounds **3h** and **3m**.

Table 2
Anti-cancer activity of compounds **3h** and **3m.**

S. No.	Sample	Cytotoxicity at time (h)	IC_{50}* (µg/mL) ± SD in different cell lines		
			Jurkat (Leukaemia) Cell line	A549 (Lung) Cell line	MCF-7 (Breast) Cell line
1	**3h**	24 h	77.74 ± 1.21	90.82 ± 1.25	89.90 ± 1.27
		48 h	75.01 ± 1.36	85.31 ± 1.42	84.18 ± 0.85
		72 h	70.90 ± 1.14	79.34 ± 0.87	79.13 ± 1.41
2	**3m**	24 h	75.72 ± 1.36	86.91 ± 1.16	–
		48 h	70.17 ± 0.85	80.29 ± 0.73	–
		72 h	65.56 ± 0.75	74.28 ± 1.28	–
3	**Imatinib**	24 h	3.46 ± 1.57	2.84 ± 0.37	6.12 ± 1.05
		48 h	3.13 ± 1.47	2.62 ± 1.29	5.80 ± 0.26
		72 h	2.91 ± 0.82	2.43 ± 0.78	5.57 ± 0.92

* Each value indicate three replicates.

amino acid, hydrophobic interaction with LEU64, LEU59, MET56, ASP147, VAL65, ALA146, LEU136, THR81, LYS37, GLU52 and VAL22 amino acids of the protein. Hence, the results proved that the compound **3h** with dimethylamino substitution at the para position on the B ring of chalcone, compound **3m** with methoxy substitution at the meta and para positions on the B ring of chalcone were found to have the moderate binding efficiency in the active pockets of the target protein. It indicates that the derivatives with methyl group substitution on the B ring of chalcone has the capability to moderately fit into active pocket of protein when compared to standard drug Imatinib and there may be a chance of compounds with more number of hydrophobic substitutions on the B ring of chalcone may increase the binding interaction with protein (Table 1).

3.2.2. In vitro anticancer activity

Based on the results of *in-silico* studies, it has been observed that the compounds (**3a-m)** might possess moderate to potent cytotoxic activity. Hence, the aim of our study is to validate the *in-silico* cytotoxic studies with the *in vitro* human anti-cancer activity against the human cancer cell lines A549 (Lung), Jurkat (Leukemia) and MCF-7 (Breast). Compounds **3a-m** were screened for anticancer activity by *in-vitro* method using Morphology and MTT assay (Balakrishna and Kumar, 2015). The morphological evaluation was performed for the compounds **3a-m** against three human malignant cell lines (Jurkat, A549 and MCF-7). Compound **3h** had shown moderate cellular changes like rounding, vacuole formation against A549 and shrinking, abnormal rounding against MCF-7 and shrinking, blebbing against Jurkat cell line at both the concentrations tested (75 & 150 μg/mL) (Balakrishna and Kumar, 2015). Compound **3m** shown moderate cellular changes like rounding, vacuole formation against A549, and shrinking, abnormal rounding against MCF-7, but doesn't show any significant cellular changes against Jurkat cell line at both the concentrations tested (75 & 150 μg/mL). Microscopic images are depicted in Fig. 3. Based on the Morphological studies, we conducted the MTT assay for **3h** against Jurkat, A549, and MCF-7 and **3m** against Jurkat and A549 human cell-lines. The IC_{50} values were determined by Non-linear regression method and presented in Table 2.

Compound **3h** which has a dimethylamino group at the para position in aromatic portion showed cytotoxic activity against three human cell lines Jurkat, A549 and MCF-7 with IC_{50}values of 70.90, 79.34, and 79.13 μg/mL respectively. Compound **3m** which has 3, 4, 5-trimethoxy substitution in aromatic portion showed cytotoxic activity against two human cell lines Jurkat and A549 with IC_{50} values of 65.56 and 74.28 μg/mL. Results indicating that the cytotoxic activity of compound **3h** and **3m** was less when compared to standard drug Imatinib which has potent cytotoxic activity against three human cell lines Jurkat, A549 and MCF-7 with IC_{50} values of 2.91, 2.43, and 5.57 μg/mL respectively. The *in vitro* MTT assay results were found to be in accordance with in-silico docking studies, which indicates that compound **3h** and **3m** possess less cytotoxic activity when compared with standard drug Imatinib.

Moreover, when the cell lines subjected to the compounds **3h** and **3m** were observed under the microscope, it was evident that the compounds caused skunking and blebbing of cells, which leads to the cell death. Vacuoles were formed in cells A549 which lead to cell death, cell deformities induced in the cells tested by the compounds **3h** and **3m** is indicated by arrows.

4. Conclusion

Some new coumarinylchalcones derivatives (**3a-m)** were synthesized and evaluated for anticancer activity. The *in silico* docking results described that the derivatives with dimethylamino substitution at para position (**3h)** and 3, 4, 5 trimethoxy substitution (**3m**) on B ring of chalcone moiety shows good binding energies. Further *in vitro* anticancer activity was performed using MTT assay methods for compound showing good results in *in silico* studies. Morphology evaluation indicates that the compound **3h** is potent against all three human malignant cell lines A549 (Lung), Jurkat (Leukemia) and MCF-7 (Breast), while compound **3m** is moderate against only two human malignant cell lines A549 (Lung) and Jurkat (Leukemia). MTT assay indicates that the compound **3h** is potent against all three human malignant cell lines A549 (Lung), Jurkat (Leukemia) and MCF-7 (Breast) with IC_{50} values as 70.90, 79.34 79.13 μg/mL respectively. The compound **3m** showed moderate activity against two human malignant cell lines A549 (Lung) and Jurkat (Leukemia) with IC_{50} values as 65.56 and 74.28 μg/mL. Future research is required to explain the mechanism of action for anti-cancer activity.

Declaration of Competing Interest

The authors declare that they have no known competing financial interests or personal relationships that could have appeared to influence the work reported in this paper.

Acknowledgments

The authors extend their appreciation to the Deanship of Scientific Research at King Saud University for funding this work through the research group project No. RG-1440-068. The authors thank the University grant commission, Delhi, India, Acahrya Nagarjuna University College of Pharmaceutical Sciences, Acharya Nagarjuna University, Guntur, VLife MDS and PGP Life Sciences, Hyderabad.

References

Anand, P., Singh, B., Singh, N., 2012. A review on coumarins as acetylcholinesterase inhibitors for Alzheimer's disease. Bioorg. Med. Chem. 20 (3), 1175–1180.
Awan, Z., Kutbi, H.I., Ahmad, A., Syed, R., Alsulaimany, F.A., Shaik, N.A., 1908. Molecular design, synthesis and biological characterization of novel Resveratrol derivative as potential anticancer agent targeting NF-κB. J. Appl. Biomed. 17.
Baek, N.-I., Ahn, E.-M., Kim, H.-Y., Park, Y.-D., 2000. Furanocoumarins from the root of Angelica dahurica. Arch. Pharmacal. Res. 23 (5), 467–470.
Balakrishna, A., Kumar, M.H., 2015. Evaluation of synergetic anticancer activity of berberine and curcumin on different models of A549, Hep-G2, MCF-7, Jurkat, and K562 cell lines. Biomed. Res. Int.
Beena, K., Suresh, R., Rajasekaran, A., Manna, P., 2016. Dihydropyrimidinones-a versatile scaffold with diverse biological activity. J. Pharm. Sci. Res. 8, 741.
Chen, Y., Wang, S., Xu, X., Liu, X., Yu, M., Zhao, S., Liu, S., Qiu, Y., Zhang, T., Liu, B.-F., Zhang, G., 2013. Synthesis and Biological Investigation of Coumarin Piperazine (Piperidine) derivatives as potential multireceptor atypical antipsychotics. J. Med. Chem. 56 (11), 4671–4690.
Di Carlo, G., Mascolo, N., Izzo, A.A., Capasso, F., 1999. Flavonoids: Old and new aspects of a class of natural therapeutic drugs. Life Sci. 65 (4), 337–353.
Ghate, M., Kusanur, R., Kulkarni, M., 2005. Synthesis and in vivo analgesic and anti-inflammatory activity of some bi heterocyclic Coumarin derivatives. Eur. J. Med. Chem. 40, 882–887.
Intekhab, J., Aslam, M., 2009. Isolation of a flavonoid from Feronia limonia. J. Saudi Chem. Soc. 13, 295–298.
Jameel, E., Umar, T., Kumar, J., Hoda, N., 2016. Coumarin: a privileged scaffold for the design and development of antineurodegenerative agents. Chem. Biol. Drug Des. 87, 21–38.
Kamal, A., Adil, S., Tamboli, J.R., Siddardha, B., Murthy, U., 2009. Synthesis of coumarin linked naphthalimide conjugates as potential anticancer and antimicrobial agents. Lett. Drug Des. Discov. 6, 201–209.
Kamal, A., Adil, S.F., Tamboli, J.R., Siddardha, B., Murthy, U.S.N., 2010. Synthesis of cyclodextrin derivatives of amino-(thiazolyl) coumarins as potential antimicrobial agents. Lett. Drug Des. Discov. 7, 665–673.
Karalı, N., Kocabalkanlı, A., Gürsoy, A., Ateş, Ö., 2002. Synthesis and antitubercular activity of 4-(3-coumarinyl)-3-cyclohexyl-4-thiazolin-2-one benzylidenehydrazones. Il Farmaco 57 (7), 589–593.
Kharasch, E.D., Hankins, D.C., Taraday, J.K., 2000. Single-dose methoxsalen effects on human cytochrome P-450 2A6 activity. Drug Metab. Dispos. 28, 28–33.

Kotra, V., Ganapaty, S., Adapa, S.R., 2010. Synthesis of a new series of quinolinyl chalcones as anticancer and anti-inflammatory agents. Indian J. Chem. 49B, 1109–1116.
Madhavan, G.R., Balraju, V., Mallesham, B., Chakrabarti, R., Lohray, V.B., 2003. Novel coumarin derivatives of heterocyclic compounds as lipid-lowering agents. Bioorg. Med. Chem. Lett. 13, 2547–2551.
Paul, M.K., Mukhopadhyay, A.K., 2004. Tyrosine kinase–role and significance in cancer. Int. J. Med. Sci. 1, 101.
Piazzi, L., Cavalli, A., Colizzi, F., Belluti, F., Bartolini, M., Mancini, F., Recanatini, M., Andrisano, V., Rampa, A., 2008. Multi-target-directed coumarin derivatives: hAChE and BACE1 inhibitors as potential anti-Alzheimer compounds. Bioorg. Med. Chem. Lett. 18, 423–426.
Pingaew, R., Saekee, A., Mandi, P., Nantasenamat, C., Prachayasittikul, S., Ruchirawat, S., Prachayasittikul, V., 2014. Synthesis, biological evaluation and molecular docking of novel chalcone–coumarin hybrids as anticancer and antimalarial agents. Eur. J. Med. Chem. 85, 65–76.
Rozmer, Z., Perjési, P., 2016. Naturally occurring chalcones and their biological activities. Phytochem. Rev. 15, 87–120.
Sashidhara, K.V., Palnati, G.R., Avula, S.R., Singh, S., Jain, M., Dikshit, M., 2012. Synthesis and evaluation of anti-thrombotic activity of benzocoumarin amide derivatives. Bioorg. Med. Chem. Lett. 22, 3115–3121.
Shaik, N.A., Al-Kreathy, H.M., Ajabnoor, G.M., Verma, P.K., Banaganapalli, B., 2019. Molecular designing, virtual screening and docking study of novel curcumin analogue as mutation (S769L and K846R) selective inhibitor for EGFR. Saudi J. Biol. Sci. 26, 439–448.
Shikishima, Y., Takaishi, Y., Honda, G., Ito, M., Takeda, Y., Kodzhimatov, O.K., Ashurmetov, O., Lee, K.-H., 2001. Chemical constituents of Prangos tschimganica; structure elucidation and absolute configuration of coumarin and furanocoumarin derivatives with anti-HIV activity. Chem. Pharm. Bull. 49, 877–880.
Singh, P., Anand, A., Kumar, V., 2014. Recent developments in biological activities of chalcones: a mini review. Eur. J. Med. Chem. 85, 758–777.
Tegginamath, G., Kamble, R.R., Kattimani, P.P., Margankop, S.B., 2016. Synthesis of 3-aryl-4-({2-[4-(6-substituted-coumarin-3-yl)-1, 3-thiazol-2-yl] hydrazinylidene} methyl/ethyl)-sydnones using silica sulfuric acid and their antidiabetic, DNA cleavage activity. Arab. J. Chem. 9, S306–S312.
Vaidyanathan, V., Naidu, V., Jabed, A., Tran, K., Kallingappa, P., Kao, C.H.-J., Wang, A., Karunasinghe, N., Pallati, R., Marlow, G., Noor Ahmad, S., Ferguson, L.R., 2019. Modern molecular biology technologies and higher usability of ancient knowledge of medicinal plants for treatment of human diseases. Plant and Human Health vol. 2, 173–205.
Valente, S., Bana, E., Viry, E., Bagrel, D., Kirsch, G., 2010. Synthesis and biological evaluation of novel coumarin-based inhibitors of Cdc25 phosphatases. Bioorg. Med. Chem. Lett. 20, 5827–5830.
Venugopala, K.N., Rashmi, V., Odhav, B., 2013. Review on natural coumarin lead compounds for their pharmacological activity. Biomed. Res. Int.
Viana, J.d.O., Félix, M.B., Maia, M.d.S., Serafim, V.d.L., Scotti, L., Scotti, M.T., 2018. Drug discovery and computational strategies in the multitarget drugs era. Braz. J. Pharm. Sci., 54
Vijay, K., Ganapaty, S., Rao, A.S., 2010. Synthesis, characterization and biological evaluation of some dihydropyrimidinones. Asian J. Chem. 22, 2518.
Wang, C., Pei, A., Chen, J., Yu, H., Sun, M.L., Liu, C.F., Xu, X., 2012. A natural coumarin derivative esculetin offers neuroprotection on cerebral ischemia/reperfusion injury in mice. J. Neurochem. 121, 1007–1013.
Wei, H., Ruan, J., Zhang, X., 2016. Coumarin–chalcone hybrids: promising agents with diverse pharmacological properties. RSC Adv. 6, 10846–10860.